Materials Letters 210 (2018) 73–76

Contents lists available at ScienceDirect

Materials Letters

journal homepage: www.elsevier.com/locate/mlblue

Carbonized metal–organic frameworks nanorods as recyclable photocatalyst for visible light-induced water oxidation

Min Zhang [a], Jianmin Luo [a], Xiaoyu Liang [a], Baolin Yan [a], M.I. Baikenov [b], Xintai Su [a,*], Le Chi [a], Chao Yang [a,*]

[a] Ministry Key Laboratory of Oil and Gas Fine Chemicals, College of Chemistry and Chemical Engineering, Xinjiang University, Urumqi 830046, China
[b] Ye. A. Buketov Karaganda State University, Karaganda 470061, Kazakhstan

ARTICLE INFO

Article history:
Received 20 June 2017
Received in revised form 6 August 2017
Accepted 29 August 2017
Available online 31 August 2017

Keywords:
Fe_2C nanorods
Carbonization
MOF template
Water oxidation
Recovery

ABSTRACT

Magnetic Fe_2C nanorods were successfully synthesized by the carbonization of iron-based metal–organic framework (MOF) template and examined as photocatalyst for water oxidation reaction. An apparent turnover frequency (TOF) of $2.73 \times 10^3\ s^{-1}$ and oxygen yield of 20.64% were obtained with Fe_2C in an alkalescent aqueous solution. The rod-like Fe_2C materials is convenient to recovery and recycling of the catalyst for water oxidation. The surface conditions of the Fe_2C also remain unchanged after the photocatalytic reaction, as confirmed by X-ray photoelectron spectroscopy (XPS). Our work demonstrates that Fe_2C as efficient WOCs is a promising candidate for water oxidation.

1. Introduction

Solar-driven water-splitting has been considered as one of the major strategies for solving the global energy problem [1], which contains two process of the hydrogen evolution reaction (HER) and the oxygen evolution reaction (OER) [2]. Of these, OER is presently the least efficient because it suffers from a complex four-electron oxidation process and sluggish kinetics, requires rearrangement of multiple bonds, and finally forms two O—O bonds ($2H_2O \rightarrow O_2 + 4H^+ + 4e^-$) [3]. Catalyst development is critical to address this challenge. Hence, it is urgent to design the efficient catalysts to lower the activation barrier to produce O_2 efficiently and satisfy the requirements for the severe water oxidation conditions.

During the past decade, most studies in the field of light-driven water oxidation catalysts (WOCs) mainly is on ruthenium and Iridium complexes [4], but their finite supplies restricts their long-term application largely. In recent years, iron-based nano-material has aroused people's attention as catalyst for water oxidation, because of their potential capacity such as earth abundant, non-toxic and less expensive [5]. Various Fe-based catalysts have been studied for water oxidation, including Fe_2O_3, Fe_3O_4, FeOOH, and MFe_2O_4 (M = Co, Ni, Mg and Cu) [6]. However, their catalytic behavior is usually poor due to large size and less active sites of the materials, and the main reason is limited contact area between catalytic center and reaction mixture. Therefore, it is important to explore special structure of the catalysts to enlarge contact interface to improve the performance.

Up to now, many of the porous materials are attractive in heterogeneous catalysis, which might contribute to their larger surface areas and higher porosity [7]. Our previous work found that Fe-MOFs exhibits structure-dependent photocatalytic performance for water oxidation, but it suffers from difficulties in separation and recovery [8]. Given advantages of MOFs as templates and precursors [9], we report the Fe-MOFs-templated synthesis of magnetic Fe_2C nanorods and the application as the catalyst for visible light-induced water oxidation in the $[Ru(bpy)_3]^{2+}$-$Na_2S_2O_8$ system. The results revealed that Fe_2C nanorods with efficient catalytic performance can be recovered from reaction system with an external magnetic field. The surface properties of the Fe_2C nanorod remain unchanged after examination by XPS before and after the photocatalytic reaction.

2. Experimental section

In a typical synthesis of MIL-88B-NH_2 (Fe) ($[Fe_3O(H_2N\text{-}BDC)_3]$), 0.64 g of PluronicF127 was dissolved in 53.4 mL of de-ionized water, followed by adding 6.6 mL of 0.4 M $FeCl_3{\cdot}6H_2O$ aqueous

* Corresponding authors.
E-mail addresses: suxintai827@163.com (X. Su), jerryyang1924@163.com (C. Yang).

http://dx.doi.org/10.1016/j.matlet.2017.08.119
0167-577X/

solution. The resulting solution was stirred for 1 h, and subsequently 1.2 mL of acetic acid was injected. After 1 h, 0.24 g of H_2N-BDC (2-Amino-benzenedicarboxylic acid) was added. After further magnetic stirring for 2 h, the reaction mixture was transferred into a 100 mL Teflon-lined autoclave and heated to 120 °C for 24 h.

Rod-like Fe_2C was obtained by the pyrolysis of the as-obtained MOFs precursor. A porcelain boat loaded with MIL-88B-NH_2 (Fe) was put in the tube furnace under dynamic vacuum condition at 200 °C for 24 h. Then, the temperature was elevated to 600 °C with a ramping temperature of 1.5 °C/min and maintained for 1 h in Ar. When naturally cooled to room temperature, the black product was collected, washed and dried.

The morphologies and structures of the as-synthesized products were identified by XRD (Bruker D8 X-ray diffractometer), TEM (Hitachi H-600) and FESEM (Hitachi SU8010). The water oxidation reactions were conducted at room temperature. Desired amount of Fe_2C were added to a flask (20 mL) with 10 mL borate buffer solution containing 1.0 mM $[Ru(bpy)_3]^{2+}$ and 5.0 mM $Na_2S_2O_8$ under illumination (300 W Xe lamp: $\lambda \geq 420$ nm, 132.8 mW/cm^2). The evolved O_2 was analyzed by GC with a thermal conductivity detector (Shimadzu GC-14B).

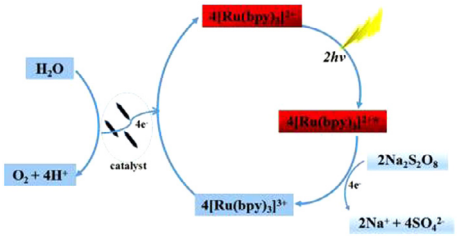

Scheme 1. The processes of photocatalytic water oxidation with $Na_2S_2O_8$ and $[Ru(bpy)_3]^{2+}$ using the Fe_2C nanorods as catalyst.

The mechanism of the visible light-driven water oxidation is depicted in Scheme 1. Firstly, $[Ru(bpy)_3]^{2+}$is photo-induced to produce $[Ru(bpy)_3]^{2+*}$ (where * denotes the excited state). Subsequently, electron transfer from $[Ru(bpy)_3]^{2+*}$ to $S_2O_8^{2-}$ leads to $[Ru(bpy)_3]^{3+}$, SO_4^{2-}. The $[Ru(bpy)_3]^{3+}$ consecutively oxidizes catalyst to high oxidation states [10], and water are oxidized to liberate O_2. In this process, it is suggested that Fe_2C facilitates the electron transfer from water to $[Ru(bpy)_3]^{3+}$.

3. Results and discussion

MIL-88B-NH_2 (Fe) was synthesized according to the previously reported literature [11], and the detailed characterization is shown in Fig. 1. The XRD pattern exhibits excellent crystalline structures (Fig. 1a), which is consistent with the previous report [12]. And a FESEM image shows that it is composed of well-defined nanorods with uniform lengths of ~300 nm and widths of ~50 nm (Fig. 1b). The TEM image further supports the SEM observation, exhibiting nanorod-like morphology with sharp tips (Fig. 1c). Fe_2C nanorods were obtained by the pyrolysis of MIL-88B-NH_2 (Fe) in Ar. XRD pattern of the sample contains peaks that can be indexed to the cambiform phase of Fe_2C (JCPDS No. 36-1249) (Fig. 1d). SEM (Fig. 1e) and TEM (Fig. 1f) images of Fe_2C nanorods show almost the same morphology as that the pristine MIL-88B-NH_2 (Fe), despite a reduction in size during the carbonization treatment. In addition, the

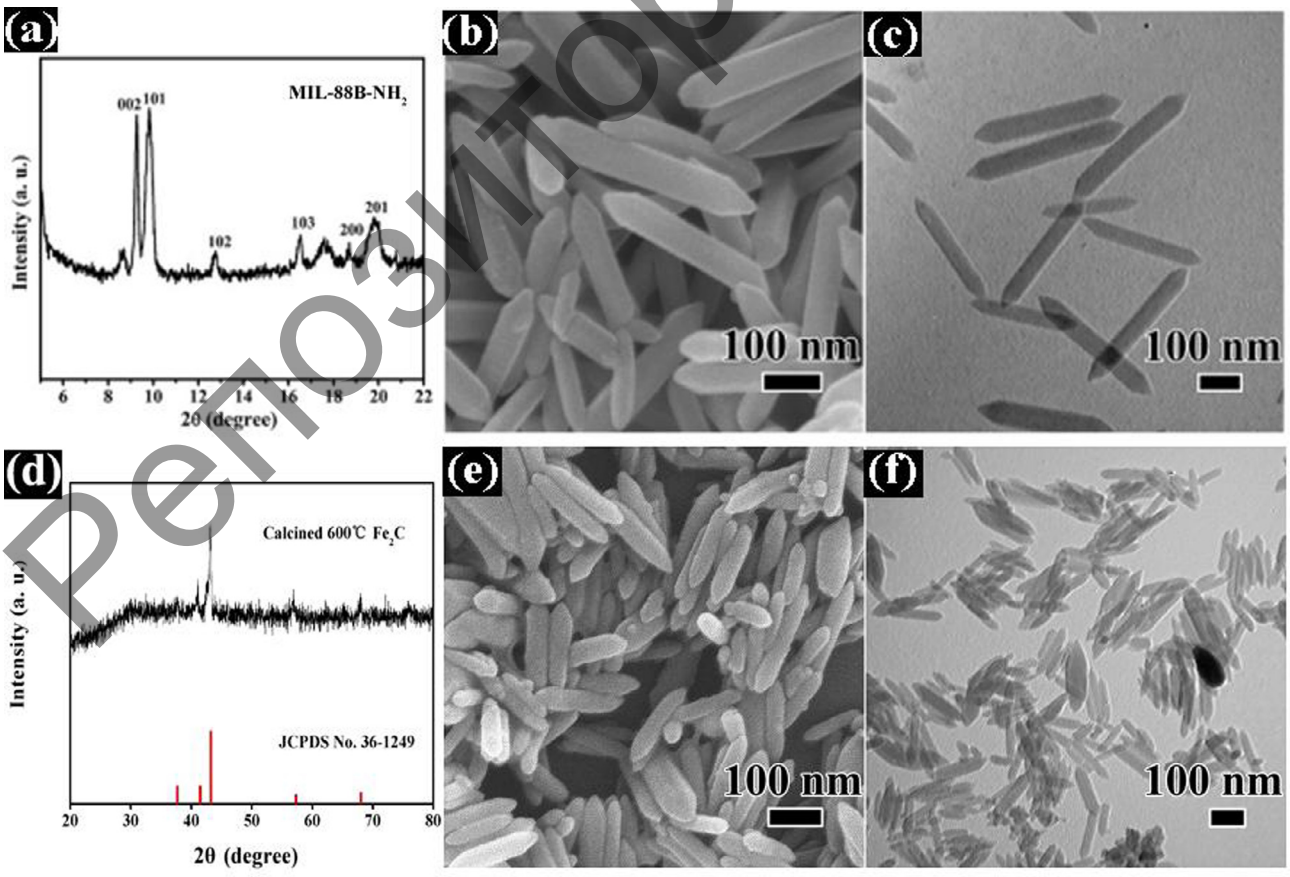

Fig. 1. (a) XRD pattern of as-synthesized MIL-88B-NH_2 (Fe); (b and c) FESEM and TEM images of nanoscale MIL-88B-NH_2 (Fe); (d) XRD pattern of Fe_2C; (e and f) FESEM and TEM images of Fe_2C.

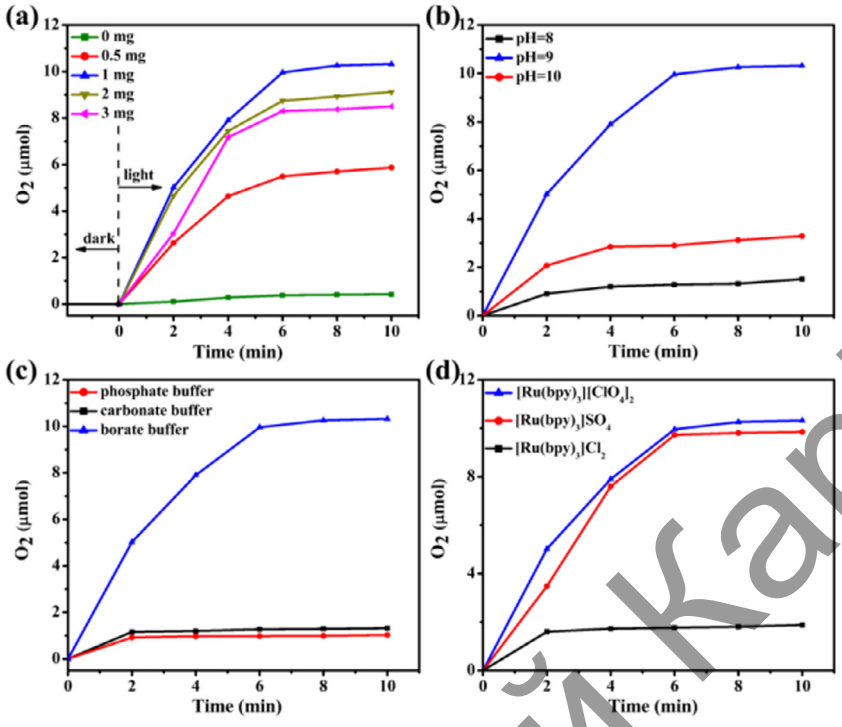

Fig. 2. Kinetics of O_2 evolution over Fe_2C under different conditions: (a) Fe_2C dosage (1.0 mM $[Ru(bpy)_3](ClO_4)_2$, 80 mM sodium borate buffer, pH = 9); (b) pH values (1 mg Fe_2C, 1.0 mM $[Ru(bpy)_3](ClO_4)_2$, 80 mM sodium borate buffer); (c) type of buffers (1 mg Fe_2C, 1.0 mM $[Ru(bpy)_3](ClO_4)_2$, pH = 9); (d) type of photosensitizers (1 mg Fe_2C, 1.0 mM photosensitizer, 80 mM sodium borate buffer, pH = 9).

detailed composition of the Fe_2C was studied by XPS and energy dispersive spectroscopy (EDS) (Fig. S1), and the binding energy of each element was further analyzed (Fig. S2).

Given to the interesting one-dimensional morphology of Fe_2C nanorods with sharp ends might be advantageous for catalysis, their catalytic performance was investigated by using water oxidation under visible light irradiation as the model reaction. To obtain the optimal conditions for water oxidation reaction, we systemically investigated a range of conditions, including catalytic amount, solution pH, buffer and type of photosensitizer (Fig. 2). Firstly, a series of experiments were carried out to study the influences of different dose of Fe_2C on catalyst water oxidation reaction. The maximum amount of O_2 evolution achieved 10.32 μmol of 1 mg Fe_2C after 10 min irradiation. Meanwhile we observed that without Fe_2C, only tiny amount of O_2 is evolved within 10 min under light irradiation (Fig. 2a). Oxygen evolution over Fe_2C is observed to be sensitive to aqueous pH, where the pH value for the optimum of O_2 generation is 9 (Fig. 2b). This is attributed to unfavorable thermodynamics for water oxidation at lower pH and the accelerated degradation of the photosensitizer at higher pH [13]. Buffers and photosensitizers also have significant influences on water oxidation over Fe_2C. The borate buffer system is more favor of water oxidation, when compared with the phosphate and carbonate buffers (Fig. 2c). The use of $(Ru(bpy)_3)(ClO_4)_2$ as the photosensitizer achieves a higher amount of oxygen evolution over Fe_2C than $(Ru(bpy)_3)SO_4$ and $(Ru(bpy)_3)Cl_2$ (Fig. 2d). In addition, the contrast experiments including the absence of illumination, electron acceptor, and photosensitizer, respectively, confirm that OER activity is closely related to reaction environment (Table S1).

Compared with the other photocatalyst, Fe_2C shows a higher initial turnover frequency (TOF = 2.73×10^3 s^{-1}) for visible light-driven oxygen evolution and a higher oxygen yield (20.64%). Table S2 displays the amount of O_2 evolution obtained from different types of Fe-based catalysts studied. The cycling stability of the Fe_2C photocatalyst was investigated by repeating water oxidation

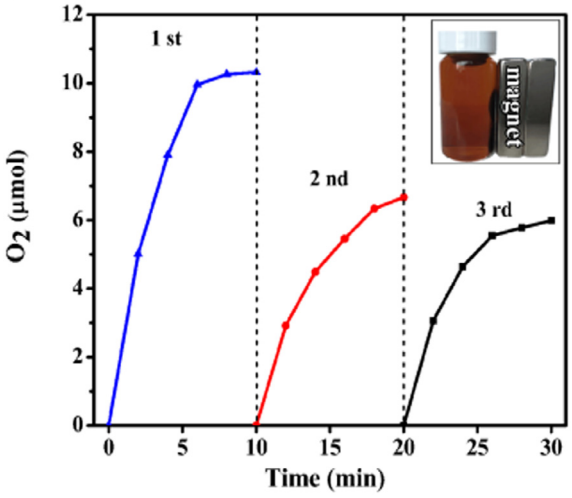

Fig. 3. Kinetics of O_2 evolution of the photocatalytic system using fresh Fe_2C and recovered Fe_2C. Conditions: 1 mg catalyst, 1.0 mM $[Ru(bpy)_3](ClO_4)_2$, 80 mM sodium borate buffer (initial pH 9.0).

tests. It can be found that the amount of O_2 evolution decreases by 39.5% at the second cycle, while the cycling system deliver a negligible fade (Fig. 3). Such decrease may be a result of the loss of catalytic particles during the recovery process. In addition, the state of Fe_2C after the OER was investigated using XRD and XPS (Fig. S3).

4. Conclusion

In summary, one-dimensional magnetic Fe_2C nanorods were successfully fabricated by a two-step method, including the syn-

thesis of MIL-88B-NH_2 (Fe) templates and subsequent thermal decomposition. The magnetic recyclable Fe_2C was used as the photocatalyst for water oxidation under alkaline conditions and exhibited good photocatalytic water oxidation activity with a TOF of 2.37×10^{-3} s^{-1}, an oxygen yield of 20.64%. Moreover, no almost changes in the surface conditions of Fe_2C before and after OER was observed by XPS.

Acknowledgement

We appreciate the financial support of the National Natural Science Foundation of China (U1503391).

Appendix A. Supplementary data

Supplementary data associated with this article can be found, in the online version, at http://dx.doi.org/10.1016/j.matlet.2017.08.119.

References

[1] S.Y. Reece, J.A. Hamel, K. Sung, T.D. Jarvi, A.J. Esswein, J.J. Pijpers, D.G. Nocera, Science 334 (2011) 645–648.
[2] J. Luo, J.H. Im, M.T. Mayer, M. Schreier, M.K. Nazeeruddin, N.G. Park, S.D. Tilley, H.J. Fan, M. Grätzel, Science 345 (2014) 1593–1596.
[3] B.M. Hunter, H.B. Gray, A.M. Müller, Chem. Rev. 116 (2016) 14120–14136.
[4] D. Hong, J. Jung, J. Park, Y. Yamada, T. Suenobu, Y.M. Lee, W. Nam, S. Fukuzumi, Energy Environ. Sci. 5 (2012) 7606–7616.
[5] J.L. Fillol, Z. Codolà, I. Garcia-Bosch, L. Gómez, J.J. Pla, M. Costas, Nat. Chem. 3 (2011) 807–813.
[6] J. Huang, X. Du, Y. Feng, Y. Zhao, Y. Ding, Phys. Chem. Chem. Phys. 18 (2016) 9918–9921.
[7] R.J. White, R. Luque, V.L. Budarin, J.H. Clark, D.J. Macquarrie, Chem. Soc. Rev. 38 (2009) 481–494.
[8] L. Chi, Q. Xu, X. Liang, J. Wang, X. Su, Small 12 (2016) 1351–1358.
[9] L. Wang, Y. Zhang, X. Li, Y. Xie, J. He, J. Yu, Y. Song, Sci. Rep. 5 (2015).
[10] M. Zheng, Y. Ding, L. Yu, X. Du, Y. Zhao, Adv. Funct. Mater. 27 (2017).
[11] M.H. Pham, G.T. Vuong, A.T. Vu, T.O. Do, Langmuir 27 (2011) 15261–15267.
[12] S. Zhao, H. Yin, L. Du, L. He, K. Zhao, L. Chang, G. Yin, H. Zhao, S. Liu, Z. Tang, ACS Nano 8 (2014) 12660–12668.
[13] Q. Xu, H. Li, L. Chi, L. Zhang, Z. Wan, Y. Ding, J. Wang, Appl. Catal. B: Environ. 202 (2017) 397–403.